Asymmetry in the *LC* resonance characteristic in dc superconducting quantum interference devices: New method of observing pair-quasiparticle interference in superconducting tunnel junctions

Y. Song

Electronics Research Laboratory, The Aerospace Corporation, P.O. Box 92957, Los Angeles, California 90009

(Received 22 December 1980)

The *LC* (inductance-capacitance) resonance phenomenon in the dc SQUID (superconducting quantum interference device) creates a current peak in the *I-V* characteristics at a voltage determined by the resonance frequency. These *I-V* characteristics have been analyzed with the resistively shunted Josephson-junction model in the low-damping and small-oscillation regime. The resonance *I-V* characteristics contain sufficient information to determine all circuit parameters for the dc SQUID's. Specifically, we can apply this analysis to symmetric, tunnel-junction dc SQUID's to deduce the pair-quasiparticle interference conductance ($\cos\theta$ term).

One of the fundamental issues which have not yet been resolved in the superconductor tunneling phenomenon is the phase-dependent, pair-quasiparticle interference conductance ($\cos\theta$ term). This term arises from the modulation of quasiparticle currents by coherence effects. The tunneling Hamiltonian method applied to the superconductor-barrier-superconductor junctions yields the following tunnel currents,[1]

$$i = i_c \sin\theta + (G + G'\cos\theta)v \quad . \tag{1}$$

Here i_c is the junction critical current, θ is the difference of phases of order parameters across the junction, G and G' are the quasiparticle and interference conductances, respectively. v, the instantaneous voltage across the junction, can also be written as

$$v = \frac{\phi_0}{2\pi}\frac{d\theta}{dt} \quad , \tag{2}$$

with $\phi_0 (= 2.07 \times 10^{-15}$ V sec), the flux quantum.

The junction parameters i_c, G, and G' are temperature and voltage (frequency) dependent.[2] Their dependences have been evaluated in detail in the weak-coupling-limit BCS theory.[3] The theoretical predictions of i_c and G have already been confirmed by experimental observations.[4] There are substantial differences, however, between experimental results and theoretical predictions for G', and, therefore, the interference conductance is still of great interest.[5]

Let us summarize the present status of our knowledge on the interference conductance, both theoretical and experimental. For the tunnel junctions with identical superconductors on both sides of the barrier, on which most of the experiments have been performed, the theoretical variations of the conductance ratio $\alpha (\equiv G'/G)$ with voltage and temperature are shown qualitatively in Figs. 1(a) and 1(b), together with the scatter in experimental data in the

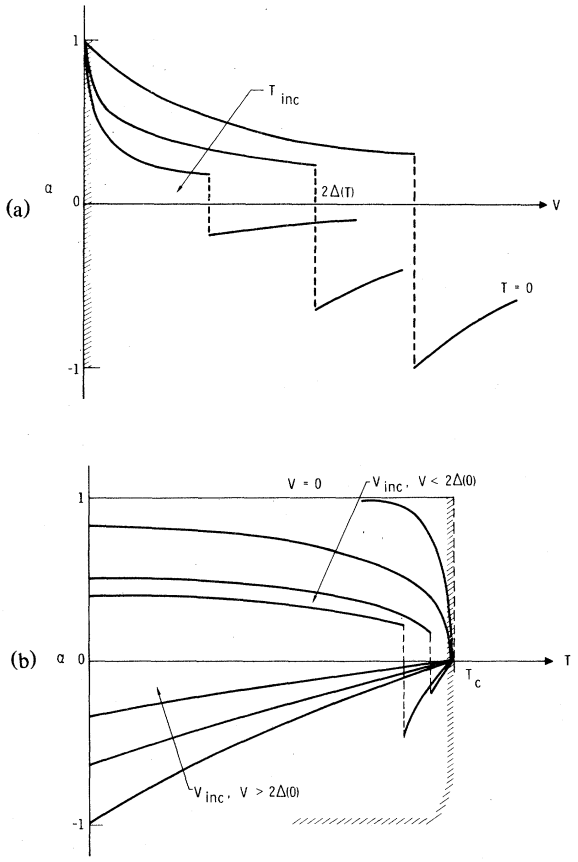

FIG. 1. (a) Theoretical α as a function of voltage at constant temperatures, and (b) theoretical α as a function of temperature at constant voltages. Hatched area is where experimental data are scattered. The arrows labeled T_{inc} and V_{inc} indicate the increasing direction of temperature and voltage, respectively.

hatched area. Figure 1(a) shows $\alpha(v)$ at constant temperature. α is 1 at $v=0$, decreases monotonically with a positive curvature up to $v=2\Delta(T)$ the energy gap at T, where it jumps discontinuously to a negative value, and thereafter approaches zero asymptotically as v is increased. The arrow indicates the increasing direction of temperature. Figure 1(b) shows $\alpha(T)$ at constant voltage. For $v<2\Delta(0)$, α starts from somewhere between ~ 0.3 and 1 at $T=0$, determined from the zero-temperature curve in Fig. 1(a), and decreases gradually with increasing T but remains positive until such a temperature is reached that $v=2\Delta(T)$. It makes a discontinuous jump to a negative value at this temperature, and approaches zero as T is further increased toward T_c, the transition temperature. For $v>2\Delta(0)$, α starts from a negative value at $T=0$ and approaches zero monotonically as T is increased toward T_c. The arrows indicate the increasing direction of voltages. In all cases, α is bounded by $|\alpha|\leq 1$.

The Josephson plasma oscillation seems to have been the only available experimental method to measure the interference conductance term in the tunnel junctions. All the reported experimental works[6–8] have used the plasma resonance. In this method a junction is biased with a dc current below i_c, so that a definite phase difference is maintained across the junction at zero dc voltage. A weak rf signal is then applied to the junction to excite a small-amplitude phase oscillation, and the junction rf responses are measured. Only a very narrow region around zero voltage can be accessed by this method. The hatched areas in Figs. 1(a) and 1(b) denote the region where the experimental data points are scattered. Only in an extremely narrow temperature region just below T_c, typically $0.98\leq T/T_c\leq 1$, is there an agreement between theory and experiment. In other regions, they are completely opposite, theory predicting $\alpha\simeq 1$ and experiment finding $\alpha\simeq -1$. Even in the papers[7,8] that reported good agreement in this narrow temperature range, there is a significant difference in the method they used to analyze the data. One used a constant G,[7] while the others used a rapidly varying $G(T)$ near T_c.[8] Since all these experiments[6–8] were done in the zero dc voltage limit, there is an intrinsic difficulty in defining G, because of its logarithmic singularity at $v=0$. Consequently it is desirable to do the measurements at finite voltage. In addition, there are practical difficulties in rf experiments in accounting for parasitic or spurious impedance contributions. In the nontunneling type of weak links, it has also been shown experimentally that $\alpha\simeq -1$.[9] Theoretical justifications have been made to show that $\alpha\simeq -1$ in these weak links,[10] but these theories are essentially different from the microscopic tunneling theory, and, therefore, have no impact on the tunnel junctions. The discrepancy in the sign of α between theory and experiment in tunnel junctions throughout most of the temperature range is interesting and has to be resolved.

We propose a new experimental method to measure this interference conductance in tunnel junctions at finite voltage. This method used the inductance-capacitance (LC) resonance phenomenon in the dc superconducting quantum interference device (SQUID), whose equivalent circuit in the resistively shunted Josephson-junction (RSJ) model is shown in Fig. 2. The loop inductance L and the junction capacitance C can be brought into resonance under appropriate conditions. It has been observed experimentally[11,12] that this LC resonance induces the current steps in the dc I-V characteristics of SQUIDs in much the same manner as in the Fiske steps[13] in tunnel junctions. These steps occur at integer multiples of the resonance voltage V_r, defined by the Josephson frequency-voltage relation $V_r=(\phi_0/2\pi)\nu_r$, where $\nu_r=(LC)^{-1/2}$ is the LC resonance frequency. The previous theoretical analysis of the circuit in Fig. 2, excluding the interference conductance $G'\cos\theta$, showed that the location, height, and width of the resonance-current steps are completely determined in the RSJ model by the circuit parameters L, C, G, and i_c, at the resonance voltage and, conversely, these parameters can be deduced from the experimental dc I-V curves.[12] In this paper, we include explicitly in the analysis the phase-dependent interference current term, $G'\cos\theta\, v$, as a current component in the junction, and study the resonance dc I-V characteristics.

In the RSJ model, the current through each arm of the SQUID consists of the following four terms,

$$i_{1,2}=i_c\sin\theta_{1,2}+G\left(\frac{\phi_0}{2\pi}\right)\frac{d\theta_{1,2}}{dt}+\alpha G\cos\theta_{1,2}\left(\frac{\phi_0}{2\pi}\right)\frac{d\theta_{1,2}}{dt}+C\left(\frac{\phi_0}{2\pi}\right)\frac{d^2\theta_{1,2}}{dt^2}\ , \tag{3}$$

where the subscript denotes each arm of the SQUID.

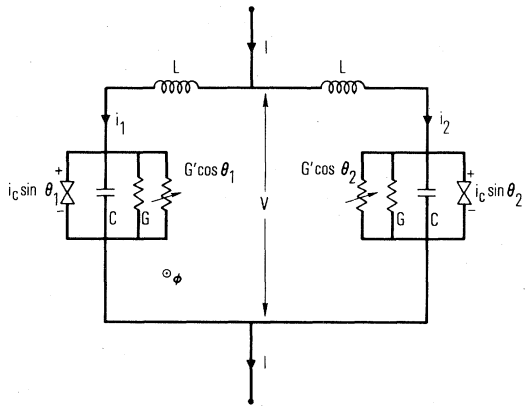

FIG. 2. Equivalent circuit of a symmetric dc SQUID with interference conductance terms.

The flux quantization around the SQUID loop requires that

$$(\theta_1-\theta_2)+\left(\frac{2\pi}{\phi_0}\right)[\phi_x+L(i_1-i_2)]=2m\pi \ , \quad (4)$$

where ϕ_x is the externally applied flux in the loop and m is an integer.[14] Equation (3) for the current-biased junctions is good only in the adiabatic regime, where the related voltages are much smaller than the gap voltage, and the voltage changes are much slower than the gap frequency. If these conditions are not saisfied, the junction currents should be described by Werthamer's equation.[15] In that case, we have a complicated integrodifferential equation[16] instead of Eq. (3), and the following analysis of LC resonance will not be possible. This effectively imposes the upper bound for the frequency (or voltage) range of our proposed experiment. In order to study the circulating current it is convenient to write equations in terms of the sum and difference of currents, i_1 and i_2, using the average phase difference $\sigma[\equiv\frac{1}{2}(\theta_1+\theta_2)]$ and the relative phase difference $\psi[\equiv\frac{1}{2}(\theta_2-\theta_1)]$ as variables. By adding and subtracting two currents, i_1 and i_2, in Eq. (3) we obtain the following equations

$$\ddot{\sigma}+\eta\dot{\sigma}+\alpha\eta(\dot{\sigma}\cos\sigma\cos\psi-\dot{\psi}\sin\sigma\sin\psi)+\tfrac{1}{2}\beta\cos\psi\sin\sigma=\sigma_x \quad (5)$$

and

$$\ddot{\psi}+\eta\dot{\psi}+\alpha\eta(\dot{\psi}\cos\sigma\cos\psi-\dot{\sigma}\sin\sigma\sin\psi)+\psi+\tfrac{1}{2}\beta\cos\sigma\sin\psi=\psi_x \ . \quad (6)$$

Here $\eta(\equiv G/\nu_r C)$ is a normalized dissipation parameter. It is the inverse of the Q of the circuit. β $[\equiv 2\pi(2L)i_c/\phi_0]$ is the usual SQUID hysteresis parameter. Time is measured in the unit of ν_r^{-1}. $\sigma_x[=\pi L(i_1+i_2)/\phi_0]$ and $\psi_x(=\pi\phi_x/\phi_0)$ are the normalized bias current and flux, respectively. These are coupled, second-order, nonlinear differential equations, for which no general solutions are available. When $|\sigma_x|\geq|\frac{1}{2}\beta\cos\psi|$ in Eq. (5), i.e., the bias current exceeds the critical current, σ will have a runaway solution, however, since there is no strong restoring force in Eq. (5). This situation corresponds to the finite-voltage state of the SQUID. Substituting such a linear solution for σ in Eq. (6), leads to a solution for ψ very similar to that of a forced, simple harmonic oscillator. It has a restoring force term ψ, and a forcing term $\frac{1}{2}\beta\cos\sigma\sin\psi$. A difference from the simple harmonic oscillator is the phase-modulated dissipation, the third term in Eq. (6). We will assume that ψ oscillates in harmonics of the forcing frequency. This corresponds to the existence of an oscillating, circulating current in the SQUID at finite voltages, a result of the flux quantization of Eq. (4).

In the following, we restrict the proposed experimental situation to a regime where $\beta\ll\eta\ll 1$. In this limit, a small oscillation approximation is valid, and the analysis is simplified. When a dc volatge V is maintained across the SQUID, the junction phase advances on the average at the rate $\nu=(2\pi/\phi_0)V$. Superimposed on this quasiconstant translation, each junction phase executes an oscillatory motion, so that we can write $\theta_{1,2}=\bar{\nu}\bar{t}+\Delta\theta_{1,2}+\theta^0_{1,2}$. Here $\Delta\theta$ is the oscillatory part and θ^0 is the flux bias angle. Bars denote that the frequency and time are measured in units of ν_r and ν_r^{-1}, respectively. This combination of translation and oscillation can be easily seen from the mechanical analog of the dc SQUID, which consists of two identical rigid pendulums connected by a torsion bar driven by a constant torque.[17] When the torque exceeds a certain critical value, the pendulums flip over the vertical axis and start to rotate. This motion is generally not uniform because an oscillation is generated by the energy exchange between pendulums and the torsion bar. Small β in the SQUID corresponds to a small moment arm of the pendulums and a large stiffness of the torsion bar. In this case the effect of gravity becomes insignificant, and an individual pendulum motion becomes independent of its angular position. The oscillatory part, $\Delta\theta$, can be expanded into a Fourier series with the fundamental frequency $\bar{\nu}$. Since the pendulums are identical, but oscillate 180° out of phase, the odd harmonics cancel each other and the even harmonics add up in the average phase difference σ. If we retain only the first harmonics in $\Delta\theta$, then $\theta=\bar{\nu}\bar{t}$ absorbing the flux bias angle $\frac{1}{2}(\theta^0_1+\theta^0_2)$ with an appropriate initial condition. When η is small, i.e., the resonance is sharp, the first harmonic is the dominant part in the circulating current, i_1-i_2, near the resonance frequency, $\bar{\nu}\simeq 1$. Since the time-dependent part of ψ is given by i_1-i_2 from Eq. (4), we write

$$\psi=\psi_0+\psi_1\cos(\bar{\nu}\bar{t}+\delta) \ .$$

We substitute these expressions for σ and ψ into Eq. (6), expand the terms into trigonometric series using Bessel-function identities, and linearize the equation in the small oscillation approximation, i.e., $|\psi_1|\ll 1$, ignoring all the higher order terms of ψ_1. Grouping dc, $\sin\bar{\nu}\bar{t}$ and $\cos\bar{\nu}\bar{t}$ terms, respectively, and equating each group to zero, we obtain the following relations:

$$\psi_1=\left(\frac{\sin^2\psi_0}{(1-\bar{\nu}^2)^2+\eta^2\bar{\nu}^2}\left[\left(\tfrac{1}{2}\beta\right)^2+\alpha^2\eta^2\bar{\nu}^2\right]\right)^{1/2} \ , \quad (7)$$

$$\delta=-\tan^{-1}\left(\frac{\eta\bar{\nu}[\frac{1}{2}\beta-\alpha(1-\bar{\nu}^2)]}{\frac{1}{2}\beta(1-\bar{\nu}^2)+\alpha\eta^2\bar{\nu}^2}\right) \ , \quad (8)$$

and

$$\psi_0 \simeq \psi_x \ . \tag{9}$$

To obtain the I-V characteristic, we turn to Eq. (5). Using the same approximations for ψ and σ, expanding in the small oscillation limit, and taking the time average, we have

$$\eta\bar{v} + \tfrac{1}{2}\beta(\tfrac{1}{2}\psi_1 \sin\delta)\sin\psi_x = \sigma_x \ . \tag{10}$$

Substituting the expressions of ψ_1 and δ from Eqs. (7) and (8) into Eq. (10), we obtain

$$\eta\bar{v} + \tfrac{1}{2}(\tfrac{1}{2}\beta)(\sin^2\psi_x)\frac{\eta\bar{v}[\frac{1}{2}\beta - \alpha(1-\bar{v}^2)]}{(1-\bar{v}^2)^2 + \eta^2\bar{v}^2} = \sigma_x \ . \tag{11}$$

This is the dc I-V characteristic of a symmetric SQUID near the LC resonance voltage in the small oscillation limit in terms of the normalized current $\sigma_x (\equiv \pi LI/\phi_0)$ and the normalized voltage $\bar{v} (\equiv V/V_r)$. The current consists of an Ohmic part, which is linear in $\bar{v}$, and a resonance part, which has a simple-harmonic-oscillator response. The first term in the resonance current is a symmetric peak about the resonance voltage, $\bar{v}=1$, and originates from the phase-independent-quasiparticle conductance G. The second term gives an antisymmetric dispersion shape and originates from the phase dependent pair-quasiparticle interference conductance G'. In Fig. 3(a), we show theoretical $\sigma_x - \bar{v}$ curves of Eq. (11) at a half flux quantum bias ($\sin\psi_x = 1$) for a few values of α, ranging from -1 to 1, in the vicinity of the resonance voltage $\bar{v}=1$. The set of parameters, $\eta=0.2$ and $\beta=0.2$, chosen for the convenience of illustration, may not be in the extreme limit of small oscillation, but reasonably well within the limit of linear regime, where $|\psi_1| \propto \beta/2\eta$ with $\alpha=0$.[12] As α changes from positive to negative, the sign of the antisymmetric component is seen to reverse. The first derivative, $d\sigma_x/d\bar{v}$, is more interesting because the Ohmic-current part becomes a constant plateau and only the resonance related features remain as shown in Fig. 3(b). The sign of α becomes readily apparent being identical to the polarity of derivative peaks. A quantitative determination of device parameters, including α, however, has to rely on fitting experimental data to theoretical curves, because at least four parameters, α, β, V_r, and η, should be determined simultaneously and self-consistently, even though G can be determined independently from the asymptotic part of the I-V curves. The step procedure which enables us in the previous work[12] to determine these parameters sequentially from experimental data is applicable if the resonance voltage V_r (or L and C) can be determined independently. To do so, we use the following measurements: The inductance L can be determined from the interference pattern $I_c(\phi_x)$ of the SQUID critical current with the applied flux.[18]

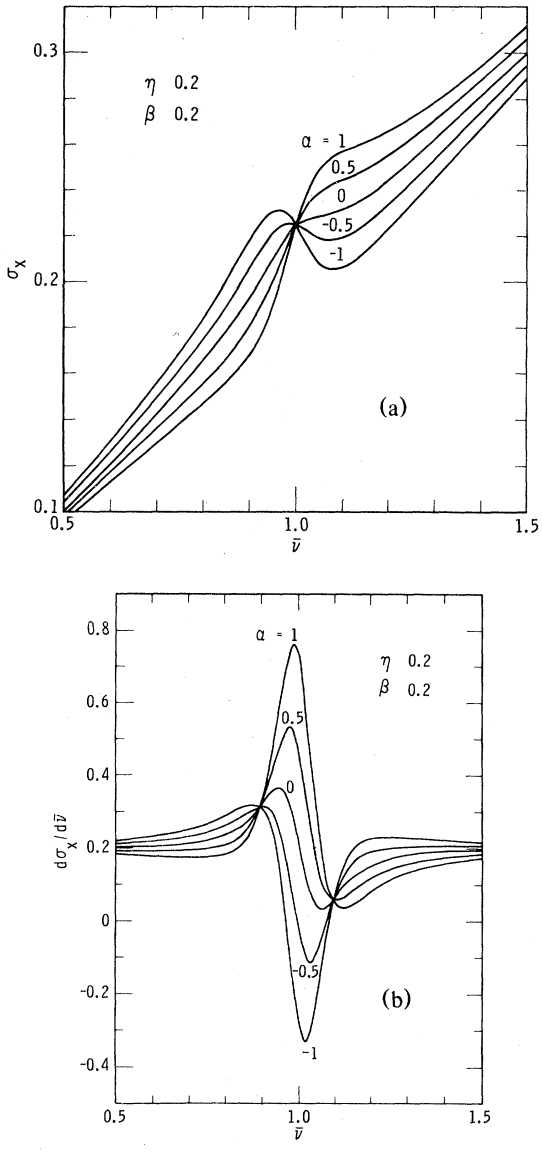

FIG. 3. (a) Theoretical σ_x-$\bar{v}$(I-V) curves showing LC resonance phenomena for various values of α, and (b) similar derivative, $d\sigma_x/d\bar{v}$-$\bar{v}$ curves.

The junction capacitance C can be calculated from the Fiske step voltages[13] and the period of modulation of junction critical current with magnetic fields. Incidentally if the applied magentic field is so large that the flux, ϕ_{xi}, linking individual junctions is not negligible, the phase difference across the junction is not uniform and the junction critical current is modulated by the Fraunhofer diffraction factor $\gamma = |\sin(\pi\phi_{xi}/\phi_0)/(\pi\phi_{xi}/\phi_0)|$. All previous equations and expressions in this work are still valid if we simply replace i_c, α, and β by γi_c, $\gamma\alpha$, and $\gamma\beta$, respectively. The proposed experimental regime

$\beta << \eta << 1$ changes to $\gamma\beta << \eta << 1$. The resonance currents are proportional to γ^2. Although inductances and capacitances determined by these methods do not give the values at the LC resonance frequency, the differences should be small enough to permit us to calculate V_r in the first approximation as long as all related frequencies are much smaller than the energy gap frequency.

Once the resonance voltage V_r is identified, we proceed as follows to determine the remaining parameters sequentially. In Fig. 4(a), an idealized, experimental I-V curve is shown. It has an asymmetric current peak centered near V_r, superimposed on an Ohmic line $I = 2GV$. The asymptotic slope should yield the quasiparticle conductance G. A steep load line should be employed to trace out a possible negative conductance reigon of the peak at $V > V_r$. The net resonance current I_r is obtained by subtracting the nonresonance current, which is Ohmic in our case ($\beta << \eta << 1$), from the total current as shown in Fig. 4 (b). Then we take halves of the sum and differences of resonance currents at $V_r \pm \Delta V$, i.e.,

$$\tfrac{1}{2}[I_r(V_r+\Delta V) \pm I_r(V_r-\Delta V)] \ .$$

These yield the symmetric part I_{rs} and antisymmetric part I_{ra} of the resonance current, respectively, as shown in Fig. 4(c). The full width at half maximum of I_{rs} is given by $\eta(=G/\nu_r C)$ from Eq. (11). Substituting the known values of G from Fig. 4(a) and ν_r into η, we then find C. The relation $\nu_r = (LC)^{-1/2}$, in turn, yields L. These L and C values have to be compared with initial trial values used in determining V_r, and adjusted in a self-consistent way. Again from Eq. (11), we derive the relation

$$I_{rs,\max} = (4\pi L/\phi_0)(i_c^2/\eta)\sin^2\psi_x \ ,$$

which enables us to determine i_c at the resonance voltage. Finally, taking the ratio of the symmetric current and the derivative of the antisymmetric current at V_r we arrive at an expression for $\alpha(=G'/G)$ from Eq. (11)

$$\alpha = \tfrac{1}{4} V_r \beta \frac{dI_{ra}}{DV} \Big/ I_{rs}\Big|_{V=V_r} \ . \tag{12}$$

The pair-quasiparticle interference conductance G' has been given in terms of all experimentally measurable quantities from a few simple measurements including I-V, $I_c(\phi_x)$ of SQUID's, $i_c(\phi_{xi})$ and the Fiske step voltages of individual junctions in the well-prepared experimental regime. Equation (12) remains same when i_c is modulated by ϕ_{xi} since both α and β should be modulated by the same factor γ.

Let us find out the sample design parameters which satisfy this regime for Pb junctions with similar geometry as our previous samples.[12] Using the relation $i_c(0) = \pi\Delta(0)G_n/2$, where G_n is the normal-state conductance, a typical capacitance value of 5×10^{-6} (F/cm^2) for Pb junctions, and scaling up the resonance frequency-dimension relation from our previous data,[12] we can rewrite $\eta = (G/\nu_r C)$ as $\eta = 0.63 i_c \nu_r/f$. Here i_c is in amperes, ν_r is in radians/sec, and f is the conductivity ratio G_n/G. The low-dissipation condition $\eta << 1$ yields $\nu_r << 1.58\times10^9 f/i_c$. In practice, $\eta \lesssim 0.2$ is sufficient to satisfy the low-dissipation condition and, therefore, $\nu_r \lesssim 0.31\times10^9 f/i_c$. The small oscillation condition, $\gamma\beta << \eta$, imposes another restriction $\nu_r >> 1.34\times10^{13}\gamma f$. A weaker condition, $\gamma\beta < \eta$, is actually good enough for this condition. We have a new combined condition, $1.34\times10^{13} \lesssim \nu_r/\gamma f \lesssim 0.31\times10^9\gamma i_c$, for Pb junctions, which requires $\gamma i_c \lesssim 23$ (μA). Let us assume a reasonable value of $\gamma f \simeq 0.1$. This sets the resonance frequency and voltage at around 200 GHz and 400 μV, respectively. At $(\phi_0/2\pi)\nu_r/\Delta \simeq 0.15$ and $(\phi_0/2\pi)G/\Delta C \simeq 0.03$

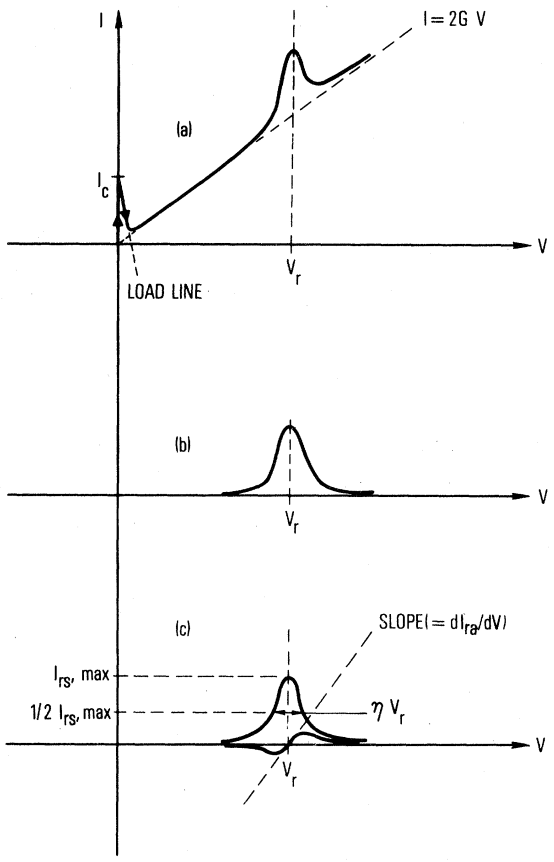

FIG. 4. Graphical illustration of determining α from I-V characteristics. (a) is the total I-V characteristic, (b) shows the net resonance current after subtracting the Ohmic current, and (c) shows decomposition of the resonance current into a symmetric and antisymmetric part.

for these samples, the adiabatic approximation of RSJ model is expected to be good within a few percent limit.[16] Scaling from our previous data,[12] this resonance frequency requires 3×3 μm^2 junctions with 16-μm separation. The corresponding, magnetic-field-modulated critical current density, γj_c, would be ~ 250 (A/cm^2). If we take $f \simeq 2$ for small voltages, for example, then $\gamma \simeq 0.05$ and $j_c \simeq 5 \times 10^3$ (A/cm^2). These dimensions and current densities are achievable with current lithographic and oxidation techniques, although not trivial.[19] If we relax the small signal requirement, we can enjoy much less stringent conditions on the experimental design at the expense of numerical computations.

The $\cos\theta$ term is virtually the last, unresolved fundamental issue in the physics of the Josephson junction. Aside from this fundamental issue, it should also play an imporant role in some applications. For instance, the ultimate performance of Josephson logic devices with respect to the power-delay product will come from the SQUID devices operating at single flux quantum levels. The $\cos\theta$ term is one of the contributing factors to the switching dynamics of these devices. The LC resonance phenomenon in dc SQUID's provides a new approach to experimentally observe the $\cos\theta$ term. Furthermore, this method offers significant advantages over others in that the $\cos\theta$ term can be measured as a function of voltage from simple dc I-V characteristics of SQUID's and junctions.

ACKNOWLEDGMENTS

I would like to thank Professor Robert Gayley for the initial discussion which led to this problem. This work was supported by the Office of Naval Research.

[1]B. D. Josephson, Phys. Lett. 1, 251 (1962); Adv. Phys. 14, 419 (1965).

[2]V. Ambegaokar and A. Baratoff, Phys. Rev. Lett. 10, 486 (1965); 11, 104E (1965); E. Riedel, Z. Naturforsch. 19A, 1634 (1964); N. R. Werthamer, Phys. Rev. 147, 255 (1964).

[3]U. K. Poulsen, Phys. Lett. 41A, 195 (1972); Rev. Phys. Appl. 9, 41 (1974); W. Schlup, Solid State Commun. 12, 631 (1973); R. E. Harris, Phys. Rev. B 10, 84 (1974).

[4]S. Shapiro, P. H. Smith, J. Nicol, J. L. Miles, and P. F. Strong, IBM J. Res. Dev. 6, 34 (1962); M. D. Fiske, Rev. Mod. Phys. 36, 426 (1971); C. A. Hamilton, Phys. Rev. B 5, 912 (1972); S. A. Buckner, T. F. Finnegan, and D. N. Langenberg, Phys. Rev. Lett. 28, 150 (1972).

[5]For instance, see R. L. Petersen, and R. I. Gayley, Phys. Rev. B 18, 1198 (1978), and references therein for recent interest in the $\cos\theta$ term.

[6]N. F. Pedersen, T. F. Finnegan, and D. N. Langenberg, Phys. Rev. B 6, 4151 (1972).

[7]O. H. Soerensen, J. Mygind, and N. F. Pedersen, Phys. Rev. Lett. 39, 1018 (1977).

[8]S. Rudner, T. Claeson, and S. Wahlsten, Solid State Commun. 26, 953 (1978); J. Appl. Phys. 50, 7070 (1979).

[9]C. M. Falco, W. H. Parker, and S. E. Trullinger, Phys. Rev. Lett. 31, 933 (1973); D. A. Vincent and B. S. Deaver, Jr., *ibid.* 32, 212 (1974); and M. Nisenoff and S. Wolf, Phys. Rev. B 12, 1712 (1975).

[10]H. Hojgaard Jensen and P. E. Lindelof, J. Low Temp. Phys. 23, 469 (1976); B. S. Deaver, Jr., R. Rifkin, and R. D. Sandell, *ibid.* 25, 409 (1976).

[11]J. E. Zimmerman and D. B. Sullivan, Appl. Phys. Lett. 31, 360 (1977).

[12]Y. Song J. P. Hurrell, IEEE Trans. Mag. 15, 428 (1979).

[13]D. D. Coon and M. D. Fiske, Phys. Rev. 138, A744 (1965).

[14]The sign conventions are such that the positive direction of field is out of paper, and $\theta_{1,2}$ is the phase difference from top to bottom side of junctions, i.e., $\theta_{1,2} = \theta^+_{1,2} - \theta^-_{1,2}$, in Fig. 2.

[15]N. R. Werthamer, Phys. Rev. 147, 225 (1966).

[16]R. E. Harris, Phys. Rev. B 11, 3329 (1975); W. A. Schlup, *ibid.* 18, 6132 (1978).

[17]For details of mechanical analogs, see, for example, T. S. Fulton, in *Superconductor Applications: SQUID's and Machines,* edited by B. B. Schwartz and S. Foner (Plenum, New York, 1977), p. 125.

[18]For instance, see R. de Bruyn Ouboter and A. Th. A. M. de Waele, in *Progress in Low Temperature Physics,* edited by C. J. Gorter (North-Holland, Amsterdam, 1969), Vol. VI.

[19]For instance, see, R. E. Harris and C. A. Hamilton, in *Future Trends in Superconductive Electronics,* edited by B. S. Deaver, C. M. Falco, J. H. Harris, and S. A. Wolf, AIP Conf. Proc. No. 44 (AIP, New York, 1978), p. 448, and references therein.